Langmuir Article

pubs.acs.org/Langmuir

Dye Sensitized Solar Cells: TiO_2 Sensitization with a Bodipy-Porphyrin Antenna System

Chang Yeon Lee and Joseph T. Hupp*

Department of Chemistry, 2145 Sheridan Road, Northwestern University, Evanston, Illinois 60208

Received August 26, 2009. Revised Manuscript Received October 19, 2009

A zinc porphyrin derivative (**2**) and zinc porphyrin−bodipy dyad (**3**) have been prepared and applied to dye-sensitized solar cells (DSSCs). On the basis of absorption and fluorescence excitation spectra, dyad **3** efficiently transfers energy from the bodipy to zinc porphyrin constituent. The **3**-sensitized solar cell demonstrates higher solar spectral coverage, based on incident photon to current efficiency (IPCE) spectra, and an improved power conversion efficiency (η = 1.55%) compared to that of the **2**-sensitized cell (η = 0.84%). The better performance of the **3**-sensitized cell is attributed largely to the gain in spectral absorbance provided by the bodipy constituent of **3**. Also evident, however, are secondary effects reflecting (a) fill-factor improvement and (b) a slight gain in porphyrin red-edge absorbance due to bodipy-conjugate formation.

Introduction

Dye-sensitized solar cells (DSSCs) have received considerable attention as a low cost alternative to conventional silicon based solar cells.[1] These photoelectrochemical cells employ molecular dyes to sensitize high-surface area, mesoporous photoelectrodes consisting of transparent semiconducting materials such as TiO_2, SnO_2,[2] ZnO,[3] and Nb_2O_3.[4] The most efficient solar cells to date are ca. 11% efficient.[5] Efforts to improve cell efficiencies have focused on the three major components of DSSCs: the dye, the redox shuttle and the semiconducting electrode.[6] In particular, efforts to develop new, improved dyes have investigated modified ruthenium polypyridyl complexes[7] and numerous organic dyes[8] including porphyrins.[9] Porphyrin derivatives are particularly attractive as sensitizers in DSSCs due to their structural similarity to chlorophylls in natural photosynthetic systems as well as their strong and tunable visible absorption properties. However, most porphyrin based cells display lower performance than ruthenium polypyridyl complex based cells despite the similar charge transfer kinetics[10] of the two systems. The inferior performance of porphyrin dyes is attributed, in part, to I_3^-−porphyrin complex formation that increases the concentration of redox shuttle at the semiconductor surface, accelerating charge interception of injected electrons by the redox shuttle (with consequent lowering of photovoltages), and quenching of a fraction of the photoexcited dyes before injection can occur (with consequent lowering of photocurrent).[11] Additionally, porphyrin absorption spectra, though strong in the Q and B band regions, are typically poor matches to the overall visible-light distribution of the solar spectrum.

To address the poor solar spectral coverage, extended porphyrin π systems have been investigated by several groups. This approach can lead to significantly broadened B band and red-shifted Q-band absorptions that fill out the solar spectrum. For instance, elongation of π systems in meso- and β-naphthalene fused porphyrins improves power conversion efficiencies by 50% relative to the nonfused systems.[9b] Similarly, attaching a conjugated anchoring group at the β position of the porphyrin ring has been successfully applied to give the best performing porphyrin based cell to date (η = 7.1%).[9c,9d]

An alternative or additional approach is to introduce antenna chromophores. The boron dipyrrin (bodipy, 4,4-difluoro-4-bora-3*a*,4*a*-diaza-*s*-indacene) molecule has often been employed as an antenna light harvesting molecule, as it has numerous favorable properties, such as high fluorescence quantum yield, low rates of intersystem crossing, large molar absorption coefficients, relatively long excited state lifetimes, and excellent photostability.[12] It can also be tailored by a variety of structural substitutions to tune

*Corresponding author. E-mail: j-hupp@northwestern.edu.

(1) O'Regan, B.; Grätzel, M. *Nature* **1991**, *353*, 737–740.

(2) (a) Kamat, P. V.; Bedja, I.; Hotchandani, S.; Patterson, L. K. *J. Phys. Chem.* **1996**, *100*, 4900–4908. (b) Ferrere, S.; Zaban, A.; Gregg, B. A. *J. Phys. Chem. B.* **1997**, *101*, 4490–4493.

(3) (a) Hoyer, P.; Weller, H. *J. Phys. Chem.* **1995**, *99*, 14096–14100. (b) Rensmo, H.; Keis, K.; Lindstrom, H.; Sodergren, S.; Solbrand, A.; Hagfeldt, A.; Lindquist, S. E. *J. Phys. Chem. B* **1997**, *101*, 2598–2602.

(4) (a) Sayama, K.; Sugihara, H.; Arakawa, H. *Chem. Mater.* **1998**, *10*, 3825–3832. (b) Lenzmann, F.; Kruegar, J.; Burnside, S.; Brooks, K.; Gratzel, M.; Ruhle, S.; Cahan, D. *J. Phys. Chem. B* **2001**, *105*, 6347–6352.

(5) Nazeeruddin, M. K.; DeAngelis, F.; Fantacci, S.; Selloni, A.; Viscardi, G.; Liska, P.; Ito, S.; Takeru, B.; Gratzel, M. *J. Am. Chem. Soc.* **2005**, *127*, 16835–16847.

(6) Hamann, T. W.; Jensen, R. A.; Martinson, A. B. F.; Van Ryswyk, H.; Hupp, J. T. *Energy Environ. Sci.* **2008**, *1*, 66–78.

(7) Robertson, N. *Angew. Chem., Int. Ed.* **2006**, *45*, 2338–2345.

(8) Mishra, A.; Fischer, M. K. R.; Bäuerle, P. *Angew. Chem., Int. Ed.* **2009**, *48*, 2474–2499.

(9) (a) Campbell, W. M.; Burrell, A. K.; Officer, D. L.; Jolley, K. W. *Coord. Chem. Rev.* **2004**, *248*, 1363–1379. (b) Tanaka, M.; Hayashi, S.; Eu, S.; Umeyama, T.; Matano, Y.; Imahori, H. *Chem. Commun.* **2007**, 2069–2071. (c) Wang, Q.; Campbell, W. M.; Bonfantani, E. E.; Jolley, K. W.; Officer, D. L.; Walsh, P. J.; Gordon, K.; Humphry-Baker, R.; Nazeeruddin, M. K.; Grätzel, M. *J. Phys. Chem. B* **2005**, *109*, 15397–15409. (d) Campbell, W. M.; Jolley, K. W.; Wagner, P.; Wagner, K.; Walsh, P. J.; Gordon, K. C.; Lukas, S.-M.; Nazeeruddin, M. K.; Wang, Q.; Grätzel, M.; Officer, D. L. *J. Phys. Chem. C* **2007**, *111*, 11760–11762.

(10) Tachibana, Y.; Haque, S. A.; Mercer, I. P.; Durrant, J. R.; Klug, D. R. *J. Phys. Chem. B* **2000**, *104*, 1198–1205.

(11) (a) O'Regan, B. C.; López-Duarte, I.; Martínez-Díaz, M. V.; Forneli, A.; Albero, J.; Morandeira, A.; Palomares, E.; Torres, T.; Durrant, J. R. *J. Am. Chem. Soc.* **2008**, *130*, 2906–2907. (b) Miyashita, M.; Sunahara, K.; Nishikawa, T.; Uemura, Y.; Koumura, N.; Hara, K.; Mori, A.; Abe, T.; Suzuki, E.; Mori, S. *J. Am. Chem. Soc.* **2008**, *130*, 17874–17881. (c) Splan, K. E.; Massari, A. M.; Hupp, J. T. *J. Phys. Chem. B* **2004**, *108*, 4111–4115.

(12) (a) Haugland, R. P. *The Handbook. A guide to Fluorescent Probes and Labeling Technologies*, 10th ed.; Spence, M. T. Z., Ed.; Molecular Probes: Eugene, OR, 2005. (b) Kang, H. C.; Haugland, R. P. U.S. Patent 5,451,663; Sept 19, **1995**. (c) Burghart, A.; Kim, H.; Welch, M. B.; Thoresen, L. H.; Reibenspies, J.; Burgess, K. *J. Org. Chem.* **1999**, *64*, 7813–7819. (d) Chen, J.; Burghart, A.; Derecskei-Kovacs, A.; Burgess, K. *J. Org. Chem.* **2000**, *65*, 2900–2906. (e) Turfan, B.; Akkaya, E. U. *Org. Lett.* **2002**, *4*, 2857–2859. (f) Coskun, A.; Akkaya, E. U. *J. Am. Chem. Soc.* **2005**, *127*, 10464–10465. (g) Qin, W.; Rohand, T.; Baruah, M.; Stefan, A.; Van der Auweraer, M.; Dehaen, W.; Boens, N. *Chem. Phys. Lett.* **2006**, *420*, 562–568.

Chart 1

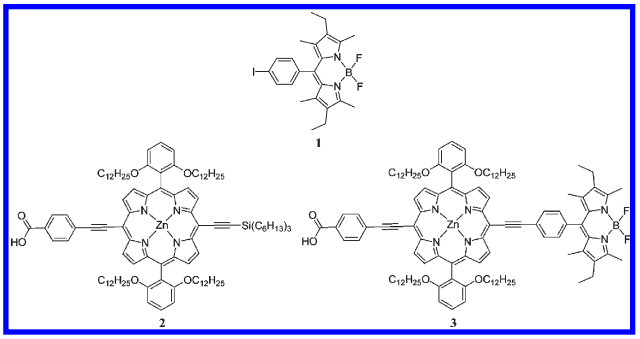

its fluorescence characteristics, allowing development of several applications in the fields of biological labeling,[13] molecular wires,[14] and artificial photosynthetic systems.[15]

We herein report the details of the preparation and characterization of a new zinc porphyrin−bodipy dyad (**3**) along with zinc porphyrin derivative (**2**) and their applications in DSSCs (Chart 1). In the dyad, the accessory pigment, bodipy, can act as an antenna light harvesting molecule to fill out the blue-green region of the spectrum where porphyrin does not absorb. We find that the dyad indeed does behave as a minimalistic antenna-type chromophoric system for photoelectrode sensitization. While there exist a handful of examples of inorganic systems that function as antenna sensitizer for high-area semiconductor photoelectrodes,[1,16] organic examples thus far are rare.

Experimental Section

Materials and General Procedures. All chemicals were obtained from commercial sources and used without further purification. All of the reactions and manipulations were carried out under N_2 with the use of standard inert-atmosphere and Schlenk techniques. Solvents used in reactions were dried by standard procedures. Absorbance spectra were obtained using a Varian Cary 5000 UV−vis−NIR spectrophotometer. Steady-state fluorescence measurements were performed on a Jobin Yvon-SPEX Fluorolog-3 spectrofluorimeter. Nuclear magnetic resonance (NMR) spectra for all the synthesized compounds were recorded on a Varian INOVA 500 NMR spectrometer (499.773 MHz for ^{1}H NMR, 125.669 MHz for ^{13}C NMR). Atomic layer deposition was performed with a Savannah 100 instrument (Cambridge Nanotech Inc.). 2,6-diethyl-4,4-difluoro-1,3,5,7-tetramethyl-8-(4-iodophenyl)-4-bora-3*a*,4*a*-diazasinadcene (**1**) was synthesized according to a literature procedure.[17]

Synthesis and Characterization. *1,3-Di(dodecyloxy)benzene*. (***4***). Resorcinol (10 g, 0.0908 mol) and *n*-bromododecane (50 mL) were successively added to a stirred suspension of potassium hydroxide (40 g, 0.713 mol) in 160 mL of dimethyl sulfoxide (DMSO). The reaction was allowed to stir overnight at room temperature and was then quenched with 150 mL of water. The product was extracted with dichloromethane-(CH_2Cl_2), dried over magnesium sulfate ($MgSO_4$), and concentrated under reduced pressure. Recrystallization from hexane yielded the compound **4** as white solid (32 g, 80% yield). ^{1}H NMR ($CDCl_3$): δ 7.17 (t, J = 8.5 Hz, 1H), 6.49 (m, 3H), 3.95 (t, J = 6.5 Hz, 4H), 1.79 (m, 4H), 1.46 (m, 4H), 1.25−1.38 (br, 32H), 0.91 (t, J = 6.5 Hz, 6H). ^{13}C NMR ($CDCl_3$): δ 160.37, 129.76, 106.60, 101.36, 67.98, 31.96, 29.70, 29.68, 29.64, 29.62, 29.44, 29.39, 29.30, 26.08, 22.73, 14.17.

2,6-Di(dodecyloxy)benzenaldehyde (***5***). A three-neck flask was fitted with a pressure-equalizing addition funnel and charged with **4** (19.2 g, 0.0430 mol) and tetramethylethylenediamine (TMEDA) (8 mL) in 120 mL of diethyl ether. The solution was degassed with a stream of N_2 for 15 min and cooled to 0 °C. Under N_2, *n*-butyllithium (1.6 M solution in hexanes 0.0645 mol) was added dropwise over 20 min and allowed to stir for 3 h. After warming to room temperature, dimethylformamide (DMF) (5.3 mL) was added dropwise, and the reaction was stirred for an additional 2 h. The reaction was quenched with water, and the product was extracted with ether (3 × 150 mL), dried over $MgSO_4$, and concentrated to leave an oily residue. The product was recrystallized from hexanes to yield a white solid (16.3 g, 80% yield). ^{1}H NMR ($CDCl_3$): δ 7.35 (t, J = 10.0 Hz, 1H), 6.51 (d, J = 5.0 Hz 2H), 4.00 (t, J = 7.5 Hz, 4H), 1.80 (m, 4H), 1.44 (m, 4H), 1.25−1.38 (br, 32H), 0.87 (t, J = 5.0 Hz, 6H). ^{13}C NMR ($CDCl_3$): δ 189.20, 161.65, 135.55, 114.65, 104.43, 68.86, 31.94, 29.70, 29.66, 29.64, 29.59, 29.52, 29.47, 29.39, 29.07, 26.00, 22.71, 14.13.

meso-(2,6-Di(dodecyloxy)phenyl)dipyrromethane (***6***). **5** (4.50 g, 9.48 mmol) was added to 16.4 mL of pyrrole and degassed for 10 min with a stream of N_2. Trifluoroacetic acid (70.0 μL) was then added in a portion, and the reaction mixture was stirred at room temperature for 2 h. NaOH (1.32 g, 32.9 mmol) was added to quench the reaction, followed by additional stirring for 1 h. The reaction mixture was filtered and the volatiles were evaporated from the filtrate using a rotary evaporator. The residue was subjected to column chromatography over silica gel (hexanes/CH_2Cl_2/ethyl acetate 7:2:1 v/v/v) to yield the desired product as a slightly yellow oil (2.52 g, 45%). Compond **6** was quickly used to prepare the next porphyrin molecule without further characterization due to its instability in the air.

[*5,15-Bis(ethynyl)-10,20-bis[2,6-di(dodecyloxy)phenyl]porphinato]zinc* (***7***). Compound **6** (2.05 g, 3.47 mmol) and trimethylsilylpropynal (0.52 mL, 3.47 mmol) were added to 547 mL of dried CH_2Cl_2 and the solution was degassed for 5 min with a stream of N_2. $BF_3\cdot 2Et_2O$ (87.5 μL) was added slowly, and the reaction mixture was allowed to stir under N_2 atmosphere for 5 min at 0 °C. Then 837 mg of DDQ was added. After stirring for 30 min, 2 mL of pyridine was added. The precipitates were filtered off and the volatiles were removed under reduced pressure. The resulting residue was purified by silica-gel column chromatography (hexane/dichloromethane (1:1 v/v)) to afford pure 5,15- bis-[(trimethylsilanyl)ethynyl]-10,20-bis[2,6-di(dodecyloxy)phenyl]porphyrin, which was further metalated with zinc(II) acetate according to the literature procedure to afford [5,15-bis[(trimethylsilanyl)ethynyl]-10,20-bis[2,6-di(dodecyloxy)phenyl]porphinato]zinc. Then, 400 mg of [5,15-bis[(trimethylsilanyl)ethynyl]-10,20-bis-[2,6-di(dodecyloxy)phenyl]porphinato]zinc obtained from the above reaction was treated with TBAF (1.63 mL, 1 M in THF) in THF (25 mL) for 20 min. The reaction mixture was quenched with acetic acid (50 μL) and MeOH (100 mL). The resultant deep green crude product was purified by silica-gel column chromatography (hexane/THF (7:3 v/v)) to afford 315 mg of [5,15-bis(ethynyl)-10,20-bis[2,6-di(n-hexoxy)phenyl]porphinato]zinc (15% overall yield).). ^{1}H NMR ($CDCl_3$): δ 9.54 (t, J = 5.0 Hz, 4H), 8.78 (d, J = 5 Hz 4H), 7.62 (t, J = 7.5 Hz, 2H), 6.92 (d, J = 10.0 Hz 4H), 3.99(s, 2H), 3.76 (t, J = 5.0 Hz, 8H) 1.12−1.17 (m, 10H), 1.00−1.10 (m, 16H), 0.91 (m, 8H), 0.75−0.87 (br, 26H), 0.64 (m, 8H), 0.49 (m, 16H), 0.36 (m, 8H). ^{13}C NMR ($CDCl_3$): δ 159.97, 151.83, 150.83, 131.95, 130.68, 129.79, 120.93, 114.86, 105.09, 98.29, 86.87, 82.47, 68.57, 64.46, 31.92, 29.53, 29.44, 29.34, 29.32, 29.13, 28.79, 28.66, 25.27, 23.04, 22.73, 14.18. MS (MALDI−TOF): m/z 1310 ($M + H^+$).

(13) Martin, H., Rudolf, H., Vlastimil, F., Eds.; *Fluorescence Spectroscopy in Biology: Advanced Methods and their Applications to Membranes, Proteins, DNA, and Cells*; Springer-Verlag: Heidelberg, Germany, 2005.
(14) (a) Wagner, R. W.; Lindsey, J. S. *J. Am. Chem. Soc*. **1994**, *116*, 9759–9760. (b) Wagner, R. W.; Lindsey, J. S.; Seth, J.; Palaniappan, V.; Bocian, D. F. *J. Am. Chem. Soc*. **1996**, *118*, 3996–3997.
(15) Imahori, H.; Norieda, H.; Yamada, H.; Nishimura, Y.; Yamazaki, I.; Sakata, Y.; Fukuzumi, S. *J. Am. Chem. Soc*. **2001**, *123*, 100–110.
(16) (a) Wolpher, H.; Sinha, S.; Pan, J.; Lomoth, R.; Bergquist, J.; Sun, L.; Sundström, V.; Akermark, B.; Polivka, T. *Inorg. Chem*. **2007**, *46*, 638–651. (b) Lees, A. C.; Kleverlaan, C. J.; Bignozzi, C. A.; Vos, J. G. *Inorg. Chem*. **2001**, *40*, 5343–5349. (c) Ardo, S.; Meyer, G. J. *Chem. Soc. Rev*. **2009**, *38*, 115–164and references therein. .
(17) Coskun, A.; Akkaya, E. U. *J. Am. Chem. Soc*. **2006**, *128*, 14474–14475.

Scheme 1. Reagent and Conditions[a]

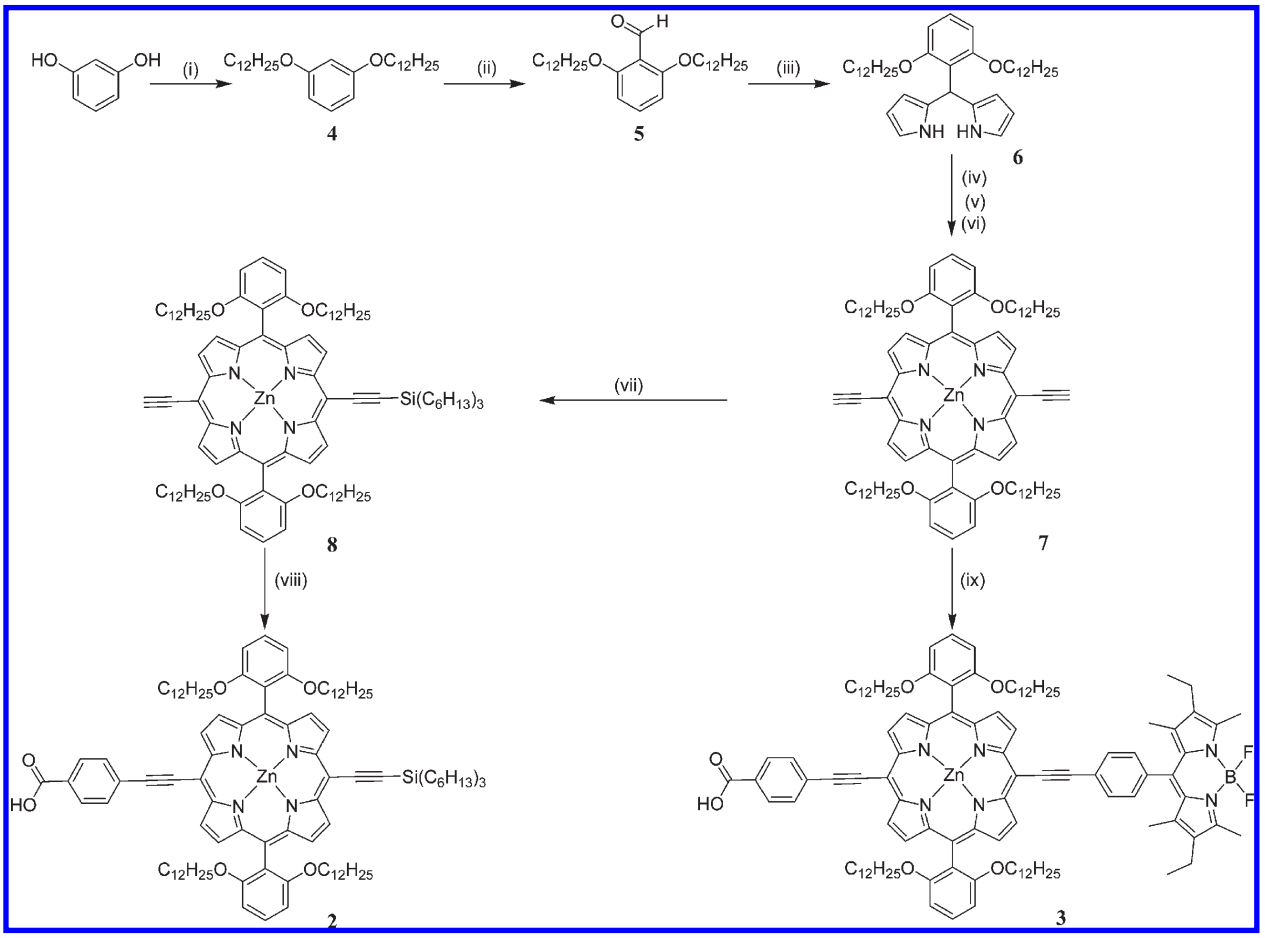

[a] Key: (i) *n*-Bromododecane, KOH, DMSO, room temperature; (ii) *n*-butyl lithium, tetramethylethylenediamine, DMF, diethyl ether, room temperature; (iii) pyrrole, TFA, room temperature; (iv) trimethylsilylpropynal, $BF_3 \cdot 2Et_2O$, DDQ, CH_2Cl_2, room temperature; (v) $Zn(OAc)_2$, CH_2Cl_2, room temperature; (vi) TBAF, THF, room temperature; (vii) *n*-butyl lithium, trihexylsilylchloride, THF, −78 °C (viii) 4-iodobenzoic acid, CuI, PPh_3, $Pd_2(dba)_3$, toluene/TEA (5:1), room temperature; (ix) **1**, 4-iodobenzoic acid, CuI, PPh_3, $Pd_2(dba)_3$, toluene/TEA (5:1), room temperature.

[*5-Ethynyl-15-*(*trihexylsilanyl*)*ethynyl-10,20-bis*[*2,6-di*(*dodecyloxy*)*phenyl*]*porphinato*]*zinc* (***8***). A solution of **7** (250 mg, 0.20 mmol) in THF (12 mL) was allowed to cool to −78 °C and *n*-BuLi (1.6 M in hexane, 125 μL, 0.2 mmol) was added slowly. After the addition was completed, the reaction mixture was allowed to warm to room temperature. After the reaction mixture was again cooled to −78 °C, trihexylsilyl chloride (88 μL, 0.24 mmol) was added dropwise. After being stirred for 15 min at −78 °C, the reaction mixture was then allowed to stir for 6 h at room temperature. The volatiles were removed under reduced pressure and the residue was extracted with CH_2Cl_2. The extract was washed with water, dried over anhydrous $MgSO_4$ and evaporated to dryness in vacuo to afford deep green oily product which was purified by silica-gel column chromatography (hexane/THF (9:1 v/v)) to afford pure [5-ethynyl-15 (trihexylsilanyl) ethynyl-10,20-bis[2,6-di(dodecyloxy)phenyl]porphinato]zinc, **8**, (143 mg, 46% yield). ^{1}H NMR ($CDCl_3$): δ 9.47 (d, J = 5.0 Hz, 2H), 9.45(d, J = 5.0 Hz, 2H), 8.69 (d, J = 10.0 Hz, 2H), 8.68 (d, J = 10.0 Hz, 2H), 7.53 (t, J = 10.0 Hz, 2H), 6.84 (d, J = 10.0 Hz 4H), 3.91(s, 1H), 3.67 (m, 8H) 1.58−1.64 (m, 6H), 1.35−1.41 (m, 6H), 1.20−1.28 (m, 12H), 0.62−1.10 (br, 75H), 0.47 (m, 8H), 0.35−0.41 (m, 8H), 0.28−0.34 (m, 8H) 0.21−0.27 (m, 8H). ^{13}C NMR ($CDCl_3$): δ 159.95, 151.90, 150.76, 150.72 132.00, 131.77, 131.00, 130.66, 129.81, 120.93, 115.00, 109.22, 105.21, 100.46, 98.65, 98.29, 86.67, 82.55, 68.68, 64.52, 33.47, 31.90, 31.73, 29.49, 29.36, 29.31, 29.23, 29.05, 28.72, 28.62, 25.24, 24.41, 23.08, 22.77, 22.71, 14.25, 14.16, 13.92. MS (MALDI−TOF): m/z 1592 (M^+)

2. A solution of **8** (102 mg, 0.064 mmol), 4-Iodobenzoic acid (17 mg, 0.070 mmol), CuI (6 mg, 0.032 mmol), and PPh_3 (16 mg, 0.064 mmol) in 10 mL of TEA/toluene (1:5 v/v) was degassed with a N_2 stream for 10 min. $Pd_2(dba)_3$ (14 mg, 0.016 mmol) was added all at once and then stirred for 12 h. Solvent was evaporated in vacuo and then dark residue was purified by silica-gel column chromatography silica-gel column chromatography (dichloromethane/methanol (95:5 v/v)) to afford pure **2**, (66 mg, 60% yield). ^{1}H NMR ($CDCl_3$): δ 9.68 (d, J = 4.5 Hz, 2H), 9.63 (d, J = 4.5 Hz, 2H), 8.91 (d, J = 4.5 Hz, 2H), 8.86 (d, J = 4.5 Hz, 2H), 8.24 (d, J = 8.0 Hz, 2H), 8.08 (d, J = 8.0 Hz, 2H), 7.73 (t, J = 8.5 Hz, 2H), 7.03 (d, J = 8.5 Hz 4H), 3.86 (m, 8H) 1.75−1.80 (m, 6H), 1.54−1.57 (m, 6H), 1.38−1.45 (m, 12H), 0.78−1.22 (br, 75H), 0.64 (m, 8H), 0.40−0.57 (br, 24H). MS (MALDI−TOF): m/z 1713 ($M + H^+$)

3. A solution of **7** (90 mg, 0.070 mmol), 4-iodobenzoic acid (19 mg, 0.076 mmol), 2,6-diethyl-4,4-difluoro-1,3,5,7-tetramethyl-8-(4-iodophenyl)-4-bora-3*a*,4*a*-diaza-sinadcene (**1**) (38 mg, 0.076 mmol) CuI (6 mg, 0.071 mmol), and PPh_3 (37 mg, 0.140 mmol) in 10 mL of TEA/toluene (1:5 v/v) was degassed with N_2 stream for 10 min. $Pd_2(dba)_3$ (32 mg, 0.035 mmol) was added all at once and then stirred for 12 h. Solvent was evaporated in vacuo and then dark residue was purified by silica-gel column chromatography silica-gel column chromatography (dichloromethane/methanol (95:5 v/v)) to afford pure **3**, (70 mg, 55% yield). ^{1}H NMR ($CDCl_3$): δ 9.82 (d, J = 4.5 Hz, 2H), 9.76 (d, J = 4.5 Hz, 2H), 9.01 (d, J = 4.5 Hz, 2H), 9.00 (d, J = 4.5 Hz, 2H), 8.28 (d, J = 7.5 Hz, 2H), 8.25 (d, J = 8.0 Hz, 2H) 8.13 (d, J = 7.5 Hz, 2H), 7.84 (t, J = 8.5 Hz, 2H), 7.61 (d, J = 8.0 Hz, 2H), 7.15 (d, J = 8.5 Hz 4H), 4.0 (t, J = 6.0 Hz, 8H), 2.70 (s, 6H), 2.47 (q, J = 6.5 Hz 4H), 1.62 (s, 6H) 1.25−1.33 (m, 8H), 1.01−1.24 (m, 38H), 0.87−0.98

(m, 20H), 0.76−0.82 (m, 8H), 0.65−0.73 (m, 16H), 0.54−0.62 (m, 8H). MS (MALDI−TOF): m/z 1808 (M^+)

Preparation of Dye-Sensitized Solar Cells. Photoelectrodes were prepared on 12 Ω cm^{-2} FTO-coated glass (Hartford glass). Blocking layers of TiO_2 were deposited using 400 ALD cycles of titanium isopropoxide (Aldrich), TIP, and water as precursors. TiO_2 was grown at 200 °C using reactant exposure times of 1 and 0.02 s for TIP and H_2O, respectively, and nitrogen purge times of 10 s between exposures. A transparent TiO_2 nanoparticle layer was prepared by doctor blading a paste of TiO_2 nanoparticles (DSL 18NR-T, Dyesol) on the FTO. A scattering layer of TiO_2 nanoparticles (WER4-O, Dyesol) was subsequently deposited on top of the transparent layer. The resulting electrodes were annealed at 500 °C in air for 30 min. The thicknesses of the photoelectrodes were approximately 12 μm, measured using a Tencor P10 profilometer. After annealing, the TiO_2 electrodes were immediately immersed in a 0.2 mM solution of **2** and **3** in THF. After 2 h, they were rinsed with THF and dried with N_2. A Surlyn frame (25 μm) was sandwiched between the open-pore side of the membrane and a platinized FTO electrode. Light pressure was applied at 130 °C to seal the cell. A solution of 0.60 M butylmethylimidazolium iodide, 0.03 M I_2, 0.10 M guanidinium thiocyanate, 0.50 M 4-*tert*-butylpyridine and 0.1 M LiI in 3 mL of acetonitrile−valeronitrile (85:15) was introduced into the TiO_2 cells. Additional Surlyn and a microscope cover slide sealed the electrolyte into the cell. Cells were illuminated through an Oriel 81092 filter using the Xe lamp and excitation monochromator of a Jobin Yvon fluorimeter. Broadband excitation using the grating at zeroth order was 98 mW cm^{-2}. Optical power was measured with an Ophir 3A-SH radiometer. A CH Instruments 1200A potentiostat was used to measure current−voltage curves.

Electrochemical Measurements. Cyclic voltammetry was carried out on a CH Instruments CH900 electrochemical analyzer using a conventional three-electrode system consisting of a platinum working electrode, a platinum wire electrode, and a pseudo Ag/AgCl reference electrode. Ferrocene/ferrocenium (+0.64 V vs NHE) was used as an internal reference. All measurements were performed at ambient temperature under nitrogen atomosphere in dry deoxygenated 0.1 M CH_2Cl_2 solution of tetrabutylammonium hexaflorophosphate.

Results and Discussion

Synthesis. The synthesis of **2** and **3** is depicted in Scheme 1 and is based on previously reported porphyrin synthetic strategies.[18] The important synthetic intermediate **7** was prepared in 15% yield from the Lewis acid catalyzed condensation of meso-substituted dipyrromethane **6** and trimethylsilylpropynal followed by Zinc metalation and deprotection of trimethylsiliyl group. Compound **8** was prepared in 46% yield by reaction between monolithiated porphyrin and trihexylsilyl chloride. Title compounds **2** and **3** were prepared in 60 and 55% yield, respectively by Pd-catalyzed Sonogashira couplings. Structures of the new compounds were characterized by various spectroscopic methods including ^{1}H NMR, ^{13}C NMR and MALDI−TOF mass spectra. The bulky alkoxyphenyl substituents were introduced at two of the four meso-positions to avoid aggregation[19] which is major factor in decreasing the efficiency of sensitized photocurrent generation.

Absorption Spectra and Fluorescence Excitation Profiles. Figure 1 shows absorption spectra and fluorescence excitation profiles of various chromophores in toluene. Compound **2** exhibits typical porphyrin absorption features with a strong Soret band at 452 nm and moderate Q bands at 582 and 639 nm. Absorption bands of compound **2** are red-shifted by 30−50 nm

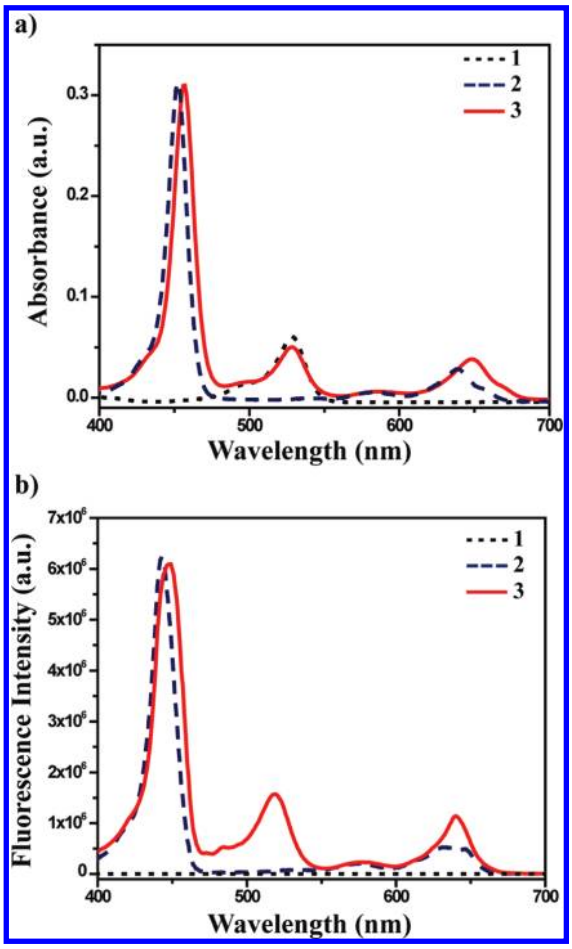

Figure 1. (a) UV−vis absorption spectra of **1**, **2**, and **3** in toluene. (b) Fluorescence excitation spectra of **1**, **2**, and **3** with fixed emission at 650 nm in toluene.

compared to those of zinc tetraphenylporphyrin in toluene,[20] reflecting extended π-conjugation. Similar results have been reported in other ethyne-linked porphyrins.[21] The spectrum of **3** exhibits characteristic absorption bands for zinc porphyrin (ZnP) (Soret band: λ_{max} = 457 nm, Q-bands: λ_{max} = 586, 648 nm) and bodipy (λ_{max} = 528 nm). The Soret band and Q-bands of **3** are red-shifted compared to those of **2**, indicating the porphyrin moiety is perturbed by the modification. Specifically, the bodipy moiety absorbs in the blue-green, a region where the porphyrin absorbs weakly. In terms of spectral coverage, this absorption enhances the light-harvesting capability of compound **3**. The fluorescence excitation spectra of compounds **1**, **2** and **3** were measured in toluene by scanning the excitation from 700 to 400 nm with fixed emission at 650 nm corresponding to ZnP. The excitation profile of **3** is well matched with its absorption spectrum, indicating that the efficient singlet-state energy transfer from bodipy to ZnP takes place in compound **3**.[22] Control experiments with **2** reveal an excitation spectrum that is well matched with its absorption spectrum, and (as expected) lacking a feature between 500 and 550 nm.

(18) Lee, C.-H.; Lindsey, J. D. *Tetrahedron* **1994**, *50*, 11427–11440.
(19) Splan, K. E.; Hupp, J. T. *Langmuir* **2004**, *20*, 10560–10566.
(20) Takahashi, K.; Komura, T.; Imanaga, H. *Bull. Chem. Soc. Jpn.* **1989**, *62*, 386–391.
(21) (a) Anderson, H. L. *Chem. Commun.* **1999**, 2323–2330. (b) Lee, C.-W.; Lu, H.-P.; Lan, C.-M.; Huang, Y.-L.; Liang, Y.-R.; Yen, W.-N.; Liu, Y.-C.; Lin, Y.-S.; Diau, E. E-G.; Yeh, C.-Y. *Chem.—Eur. J.* **2009**, *15*, 1403–1412.
(22) (a) Haugland, R. P.; Yguerabide, J.; Stryer, L. *Proc. Natl. Acad. Sci. U.S.A.* **1969**, *63*, 23–30. (b) Stryer, L.; Haugland, R. P. *Proc. Natl. Acad. Sci. U.S.A.* **1967**, *58*, 719–726. (c) Hsiao, J.-S.; Krueger, B. P.; Wagner, R. W.; Johnson, T. E.; Delaney, J. K.; Mauzerall, D. C.; Fleming, G. R.; Lindsey, J. S.; Bocian, D. F.; Donohoe, R. J. *J. Am. Chem. Soc.* **1996**, *118*, 11181–11193.

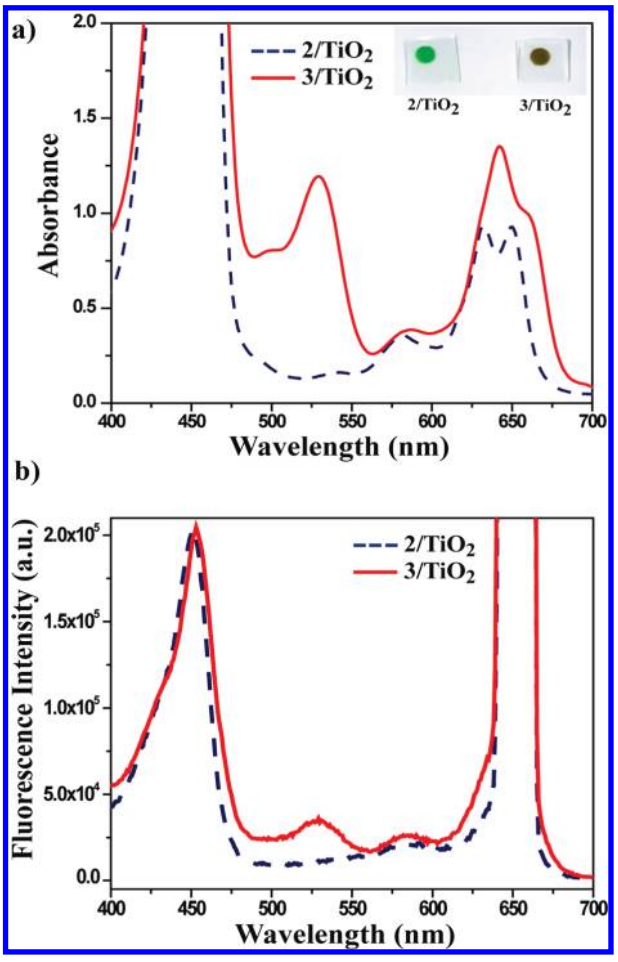

Figure 2. (a) UV−vis absorption spectra of **2** and **3** on TiO_2 and color photos of the electrods (inset). (b) Fluorescence excitation spectra of **2** and **3** with fixed emission at 650 nm on TiO_2. The intense peak between 630 and 670 nm is artifactual and arises from scattering of the excitation beam.

Absorption spectra of **2** and **3** on TiO_2 are similar to the corresponding solution spectra (Figure 2a) but exhibit a small blue shift, presumably reflecting slight aggregation.[23] To prove energy transfer from bodipy to ZnP occurs on the TiO_2 surface, fluorescence excitation spectra of **2** and **3** were measured on TiO_2 *in air* with fixed emission at 650 nm. As shown in Figure 2b, the excitation spectrum includes a feature (530 nm) assignable to bodipy absorption.

Electrochemical Properties. Electrochemical properties of **1**, **2** and **3** have been examined by cyclic voltammetric method in CH_2Cl_2 solutions with tetrabutylammonium hexafluorophosphate ($(TBA)PF_6$) as the supporting electrolyte. CVs of **1** and **2** show a reversible redox wave at 1.26 and 0.92 V vs NHE, respectively, which are obviously attributed to redox reaction at the bodipy and zinc porphyrin centers (Figure 3, parts a and b). The CV of **3** is a sum of those of **1** and **2** as expected with redox waves at 0.96 and 1.29 V vs NHE (Figure 3c). Excited oxidation potentials of **2** and **3** are calculated from the ground-state oxidation potentials, and zero−zero excitation energy E_{0-0}, according to eq 1

$$E(S^+/S^*) = E(S^+/S) - E_{0-0} \quad (1)$$

(23) (a) Akins, D. L.; Özcüelik, S.; Zhu, H.-R.; Guo, C. *J. Phys. Chem.* **1996**, *100*, 14390–14396. (b) Maiti, N. C.; Mazumdar, S.; Periasamy, N. *J. Phys.Chem. B* **1998**, *102*, 1528–1538. (c) Khairutdinov, R. F.; Serpone, N. *J. Phys. Chem. B* **1999**, *103*, 761–769. (d) Osuka, A.; Maruyama, K. *J. Am. Chem. Soc.* **1988**, *110*, 4454–4456.

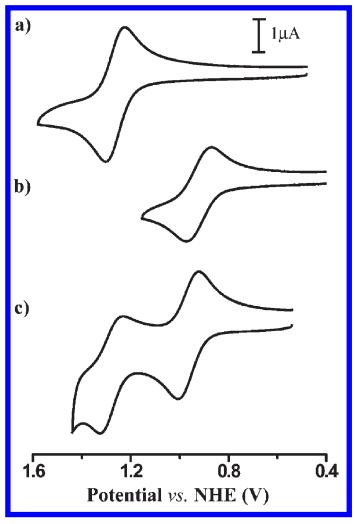

Figure 3. Cyclic voltammograms of **1** (a), **2** (b), and **3** (c) in CH_2Cl_2 containing 0.1 M $(TBA)PF_6$ (scan rate = 0.1 V/s).

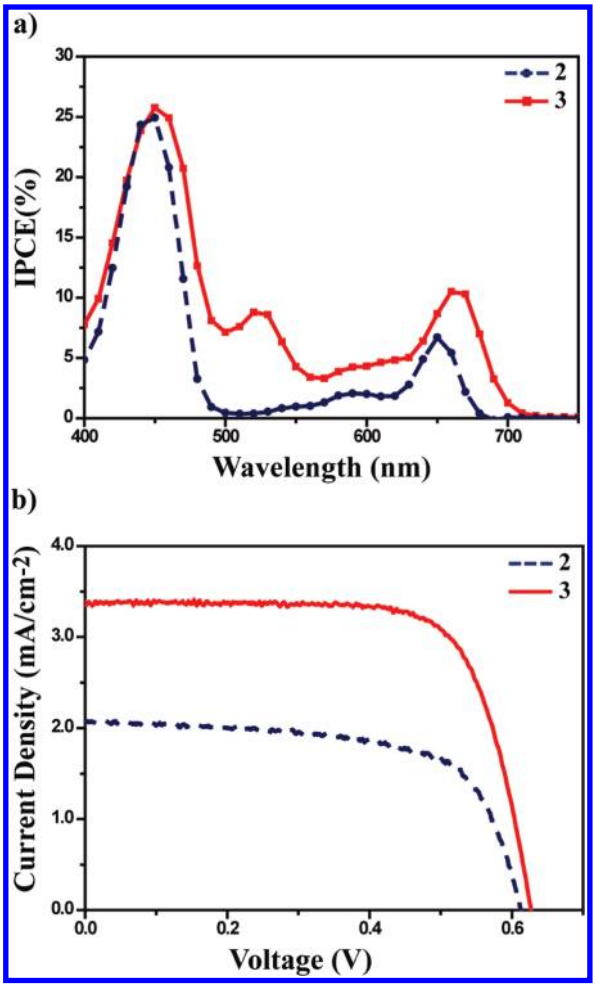

Figure 4. (a) Photocurrent action spectra of **2** and **3** sensitized solar cells (b) *J*−*V* curves of 2 and 3 sensitized solar cells under AM 1.5 illumination.

where $E(S^+/S)$ is the first oxidation potential of the sensitizer measured by cyclic voltammetry and E_{0-0} is the zero−zero excitation energy obtained by the intersection of the normalized absorption and emission spectra. The excited-state oxidation potentials of **2** and **3** are −1.02 and −0.95 V vs NHE, respectively.

These are sufficiently negative of the conduction-band-edge energy of TiO_2 in contact with the DSSC electrolyte (ca. −0.5 V vs NHE) that electron injection should be straightforward. In addition the ground- state oxidation potentials are sufficiently positive that regeneration with iodide should be both thermodynamically and kinetically feasible.

Photoelectrochemical Properties. Dye-sensitized solar cells were fabricated using **2** and **3** as photosensitizers for nanocrystalline TiO_2. A coating of 20 nm-sized TiO_2 particles was first screen-printed on a fluorine-doped SnO_2 (FTO) conducting glass electrode and then over coated with 400 nm-sized light scattering particles. The TiO_2 electrode was then immersed in **2** and **3** dye solution in THF at room temperature for 2 h. Platinized FTO conducting glass was used as counter electrode. The incident monochromatic photon-to-current conversion efficiencies (IPCEs) of cells based on **2** and **3** as sensitizers are shown in Figure 4a. The IPCE spectra are similar to the corresponding absorption spectra on TiO_2 (Figure 2a) as well as in toluene (Figure 1a). The IPCE spectrum of **3** is slightly red-shifted compared to that for **2**, consistent with the absorption spectrum of **3**. Notably, the **3**-sensitized cell shows greater solar spectral coverage compared to that of the **2**-sensitized cell with absorption between 500 and 550 nm, consistent with the notion that efficient energy-transfer-mediated electron injection is achieved by the bodipy moiety in the **3**-sensitized cell. Figure 4b shows the photocurrent−voltage (*J*-*V*) curves of the cells. Under AM 1.5 illumination, the **3**-sensitized cell exhibits a short circuit photocurrent density (J_{sc}) of 3.4 mA/cm^{-2}, an open circuit voltage (V_{oc}) of 627 mV, and a fill factor (FF) of 0.73, yielding an overall conversion efficiency (η), derived from the equation $\eta = J_{sc} \times V_{oc} \times FF$/input radiation power, of 1.55%. On the other hand, the **2**-sensitized cell gives a J_{sc} of 2.1 mA/cm^{-2}, V_{oc} of 613 mV, and FF of 0.66, yielding an η of 0.84%. The η value of the **3**-sensitized cell is nearly twice that of the **2**-sensitized cell. The higher efficiency of **3**-sensitized cell is primarily attributable to improved light harvesting by **3**.

Conclusion

A zinc porphyrin−bodipy dyad, **3,** exhibiting efficient energy transfer from the bodipy subunit to the porphyrin subunit, has been synthesized. The photovoltaic properties of **2** and **3** were evaluated by incorporation into dye sensitized solar cells. The zinc porphyrin−bodipy (**3**) dyad based cell showed nearly twice the efficiency of a zinc porphyrin (**2**) based reference cell in large part due to the improved solar spectral coverage of **3** by bodipy. Further improvement of the power conversion efficiency in porphyrin-bodipy dyad based solar cells should be possible by designing bodipy derivatives that have higher molar extinction coefficients and more red-shifted absorption.

Acknowledgment. We thank the Korean Electric Power Research Institute and the U.S. Department of. Energy's Office of Science (Grant No. DE-FG87ER13808) for support of our work. We also gratefully acknowledge support for Chang Yeon Lee via a Korea Research Foundation Grant funded by the Korean Government (MOEHRD) (KRF-2007-357-C00058).